ACS APPLIED MATERIALS & INTERFACES

Research Article

www.acsami.org

Functionalization and Reduction of Graphene Oxide with *p*-Phenylene Diamine for Electrically Conductive and Thermally Stable Polystyrene Composites

Hui-Ling Ma,[†] Hao-Bin Zhang,[†] Qi-Hui Hu,[†] Wen-Juan Li,[†] Zhi-Guo Jiang,[†] Zhong-Zhen Yu,*[,†] and Aravind Dasari*[,‡]

[†]State Key Laboratory of Organic−Inorganic Composites, Department of Polymer Engineering, College of Materials Science and Engineering, Beijing University of Chemical Technology, Beijing 100029, China

[‡]School of Materials Science & Engineering (Blk N4.1), Nanyang Technological University, 50 Nanyang Avenue, Singapore 639798

Supporting Information

ABSTRACT: A facile and efficient approach was developed to simultaneously functionalize and reduce graphene oxide (GO) with p-phenylene diamine (PPD) by simple refluxing. This was possible by the nucleophilic substitution reaction of epoxide groups of GO with amine groups of PPD aided by NH_3 solution. As a consequence, electrical conductivity of GO-PPD increased to 2.1×10^2 S/m, which was nearly 9 orders of magnitude higher than that of GO. Additionally, after the incorporation of GO-PPD in polystyrene (PS), the composites exhibited a sharp transition from electrically insulating to conducting behavior with a low percolation threshold of ~0.34 vol %, which was attributed to the improved dispersion and the reduction of GO-PPD. Thermal stability of the PS/GO-PPD composite was also ~8 °C higher than that of PS.

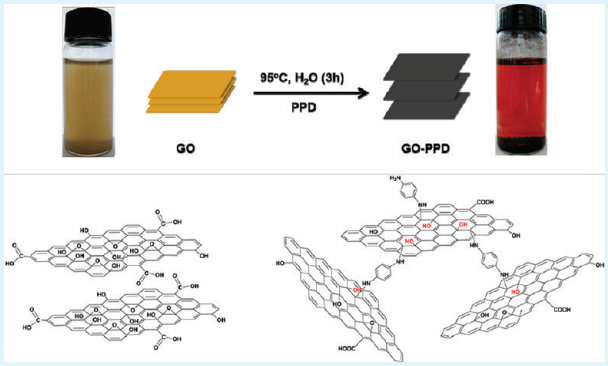

KEYWORDS: *graphene oxide, polystyrene, p-phenylene diamine, chemical reduction, electrical conductivity, thermal stability*

INTRODUCTION

Graphene has attracted wide attention because of its high electrical conductivity,[1−3] high thermal conductivity,[4−6] and superior mechanical properties.[7,8] Several methods, such as the scotch tape method,[9] chemical vapor deposition,[10,11] epitaxial growth on electrically insulating surface,[12] have been employed in preparing graphene nanosheets. However, scaling up is a major hurdle with these methods. It has been well-demonstrated that GO is an excellent precursor to prepare graphene by ultrasonic exfoliation and chemical reduction.[13−17] For example, Stankovich et al.[14] reduced ultrasonically exfoliated GO with hydrazine hydrate. Owing to the formation of unsaturated and conjugated carbon atoms, electrical conductivity of reduced GO was improved. But surface functionalization of GO prior to the chemical reduction was still necessary to prevent the aggregation of reduced GO nanosheets and improve their dispersion in polymer matrices. In view of this, Xu et al.[15] used dopamine to reduce GO with simultaneous capping by polydopamine (from self-polymerization of dopamine) to provide a versatile platform for covalent grafting of functional polymer brushes. Chen et al.[13] reduced GO with p-phenylene diamine (PPD) at 90 °C for 24 h, leading to high electrical conductivity of the reduced GO. Furthermore, the reduced GO was well-dispersed in ethanol because of its positive charge due to the adsorption of oxidized PPD. In another study, GO was functionalized based on the reaction of di-isocyanates with carboxyl and hydroxyl groups of the GO nanosheets, which effectively prevented face-to-face stacking of the nanosheets.[16] Even a pillared graphitic structure with tailored interlayer spacing was also reported by using diaminoalkanes as an intercalating and stitching agent of GO.[17]

On the basis of the above literature review, it is clear that reduction and surface functionalization of GO is important in tuning the properties that can lead to novel functional materials. In our previous investigation, we have found that octadecylamine (ODA) can simultaneously functionalize and reduce GO by simple refluxing without the use of any reducing agents.[18] Because of the reduction, electrical conductivity of GO-ODA increased to 1.2×10^{-4} S/m, which was 3 orders of magnitude higher than that of GO. Compared to ODA, PPD is expected to be more efficient in reducing and functionalizing GO as it bears two-terminal amine goups. Also, the benzene group of PPD will benefit the compatibility of GO-PPD with PS matrix. In this work, therefore, GO was simultaneously reduced and functionalized with PPD by simple refluxing.

Received: November 25, 2011
Accepted: March 15, 2012
Published: March 15, 2012

EXPERIMENTAL SECTION

Materials. Natural graphite flakes were kindly provided by Huadong Graphite Factory (China) with an average diameter of 48 μm. Fuming nitric acid (65−68%), concentrated sulphuric acid (95%-98%), hydrochloric acid (36−38%), potassium chlorate (98%), tetrahydrofuran (THF, 99.7%), methanol (99.5%), and ethanol (99.7%) were purchased from Beijing Chemical Factory (China). PPD was obtained from Tianjin Guangfu Fine Chemical Research Institute (China). PS resin with a trade name of 158 K was purchased from BASF-Yangzi Co. Ltd. (China). All the other reagents and solvents were purchased from Beijing Chemical Factory (China) and were used without further purification.

Reduction and Functionalization of GO with PPD. GO was synthesized from natural graphite by the modified Staudenmaier method.[19,20] In a typical procedure for preparing GO-PPD, GO (60 mg) was dissolved and exfoliated in 120 mL of deionized water via ultrasonication with a JY99−2 DN ultrasonicator (Ningbo, China). Subsequently, PPD (600 mg) and NH_3 solution (360 μL) were added. The mixture was refluxed with mechanical stirring at 95 °C for 3 h and filtrated with a PP membrane with an average pore size of 0.2 μm. The filtrate cake was rinsed in ethanol with the aid of ultrasonication for 5 min and then filtrated. The rinsing-filtration process was repeated for a few times to remove the physically adsorbed PPD. Finally, the filtrate cake was dried in an oven at 80 °C for 24 h.

Scheme 1. Schematic of the Reaction of GO with PPD

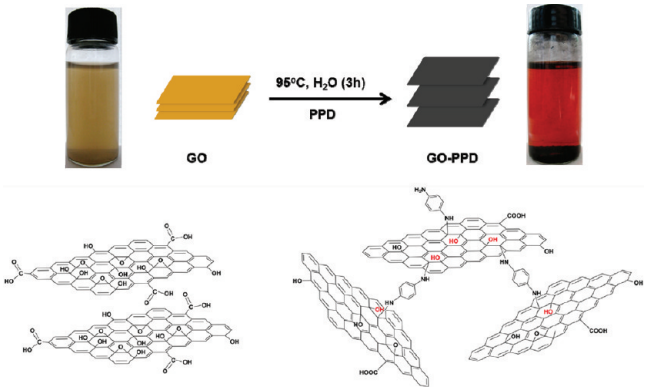

Preparation of PS/GO-PPD Composites. PS composites were prepared by solution blending. The GO-PPD or GO powder was dispersed and exfoliated in THF by ultrasonicator. The resulting suspension was mixed with PS that was dissolved in THF at 35 °C. After homogenization using an IKA T18 homogenizer (Germany) for 2 h at ambient temperature, the mixture was poured into a large volume of vigorously stirred methanol to coagulate PS composites. The precipitate was obtained by filtrating and drying successively in an air-circulating oven at 80 °C for 12 h and a vacuum oven at 80 °C for 24 h. Finally, PS/GO and PS/GO-PPD composites were compression-molded to 1 mm thick plates using a Beijing Kangsente KT-0906 vacuum hot-press (China) at 210 °C for 25 min.

Characterization. A ThermoVG RSCAKAB 250X high-resolution X-ray photoelectron spectroscopy (XPS) was used to characterize the surface compositions of GO and GO-PPD. The UV−vis absorption spectroscopy was conducted with a Hitachi UV-3010 spectrophotometer over the wavelength range from 200 to 500 nm. Atomic force microscopy (AFM) measurements were carried out with a Multimode SPM (Digital Instruments). The samples for AFM images were prepared by depositing a dispersed GO solution (0.1 mg/mL) onto a freshly cleaved mica surface and allowing them to dry in air. X-ray diffraction (XRD) spectra measurements were carried out using a Rigaku D/Max 2500 diffractometer with CuKα radiation (λ = 1.54 Å)

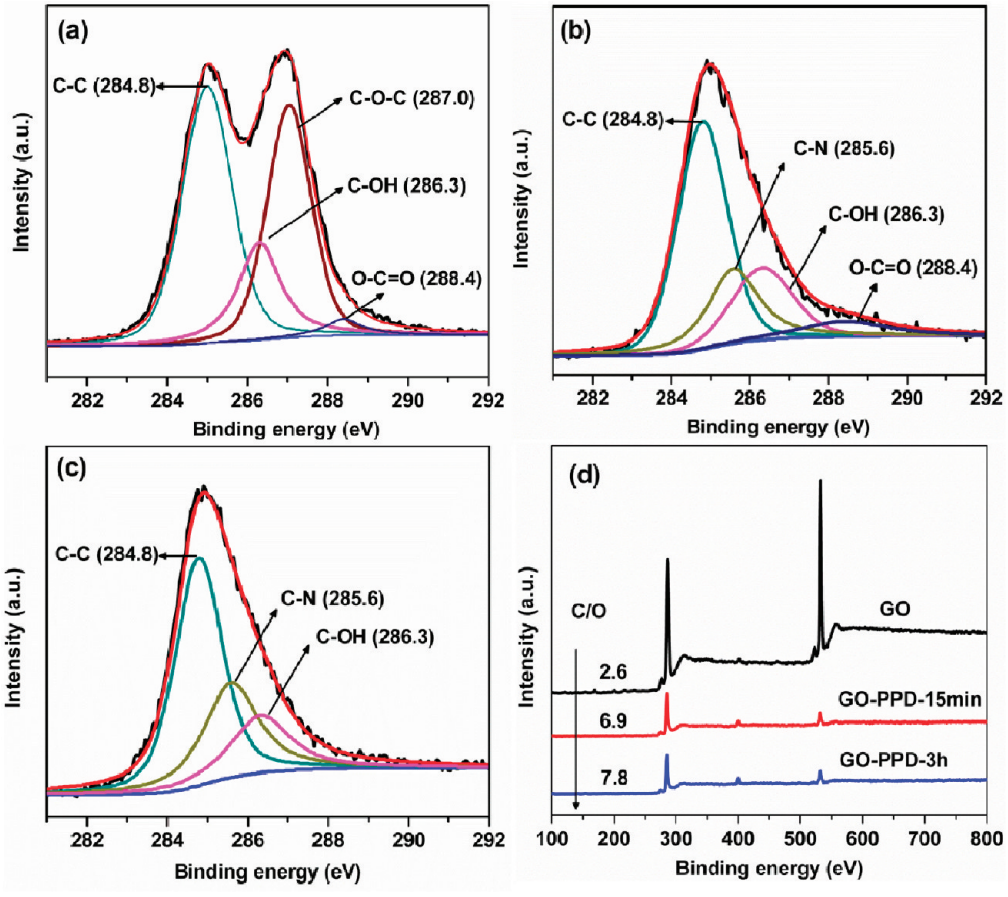

Figure 1. C 1s XPS spectra of (a) GO, (b) GO-PPD-15 min, (c) GO-PPD-3 h, and (d) general spectra.

at a generator voltage of 40 kV and a generator current of 50 mA with a scanning speed of 4°/min from 4 to 40°. GO and GO-PPD were analyzed with a Nicolet Nexus 670 Fourier-transform infrared spectroscopy (FT-IR). GO and GO-PPD films were obtained by vacuum filtration with PP membranes (an average pore size of 0.2 μm), and subsequently, dried at 80 °C for 24 h. The volume conductivities of the films were measured with a 4-Probes-Tech RTS-8 four-probe resistivity meter (China). A Hitachi S4700 field emission scanning electron microscope (SEM) was used to observe the dispersion of GO and GO-PPD in PS matrix at an accelerating voltage of 20 kV. Transmission electron microscope (TEM) observations were performed on a Hitachi H-800 electron microscope operating at an accelerating voltage of 200 kV. For TEM observations, ultrathin sections were cryogenically cut with a diamond knife using a Leica EM UC6 ultramicrotome and collected on 200-mesh copper grids. Thermogravimetric analysis (TGA) was carried out on a TA Q600 thermal analyzer under a nitrogen atmosphere at a heating speed of 10 °C/min. Volume conductivities of PS and its composites with conductivities lower than 1×10^{-4} S/m were measured by a ZC-90G resistivity meter from Shanghai Taiou Electronics (China), whereas that for materials with conductivity higher than 1×10^{-4} S/m were measured with the four-probe resistivity meter.

RESULTS AND DISCUSSION

Reduction and Functionalization of GO with PPD. GO can be dispersed well in water due to the hydroxyl, carboxyl, and epoxide groups on its surface. The average thickness of GO measured by AFM is about 0.89 nm (see Figure S1 in the Supporting Information). The functionalization of GO with PPD by the reaction between amine groups of PPD and epoxide groups of GO is shown in Scheme 1. A first indication of the reduction of GO is the color change of GO aqueous solution from brownish yellow to black after PPD was added and reacted for 15 min. XPS was used to characterize the removal of oxygen groups and the formation of chemical bonds on the surface of GO before and after its functionalization with PPD (Figure 1). As for GO, four different peaks centered at 284.8, 286.3, 287.0, and 288.4 eV are observed, corresponding to C−C in unoxidized graphite carbon skeleton, C−OH in hydroxyl group, C−O−C in epoxide group, and O−C═O in carboxyl group, respectively. After the reaction with PPD for 15 min (Figure 1b), the peaks corresponding to the oxygen-containing groups are significantly weakened, especially the peak of C−O−C in epoxide group. Accordingly, the atomic ratio of carbon and oxygen (C/O) increased from 2.6 for GO to 6.9 in GO-PPD-15 min. With increase of the reaction time to 3 h (Figure 1c), the C/O ratio increased to 7.8 (Figure 1d), indicating that most of the oxygen-containing groups are removed after the reduction. Moreover, a new characteristic peak corresponding to C−N group located at 285.6 eV appeared, suggesting that PPD is grafted onto GO nanosheets.

As shown in Figure 2a, the UV−vis spectrum of GO solution exhibits two characteristic features: a maximum at 237 nm, which can be attributed to $\pi \rightarrow \pi^*$ transition of aromatic C−C bond; and a shoulder at 302 nm corresponding to $n \rightarrow \pi^*$ transition of C═O bonds. For GO-PPD-15 min solution, the absorption peak shifted to 258 nm. With an increase in reaction time to 3 h, the peak shifted slightly to 271 nm, indicating the reduction of GO and the formation of electronic conjugation within the graphene sheets.[21,22]

The reduction of the oxygen-containing groups in GO by PPD was also confirmed by FT-IR spectroscopy (Figure 2b). As GO contains hydroxyl, carboxyl and epoxide groups, the bands at 3432 cm^{-1} and 1390 cm^{-1} are associated, respectively, with stretching and deformation vibrations of O−H bond of

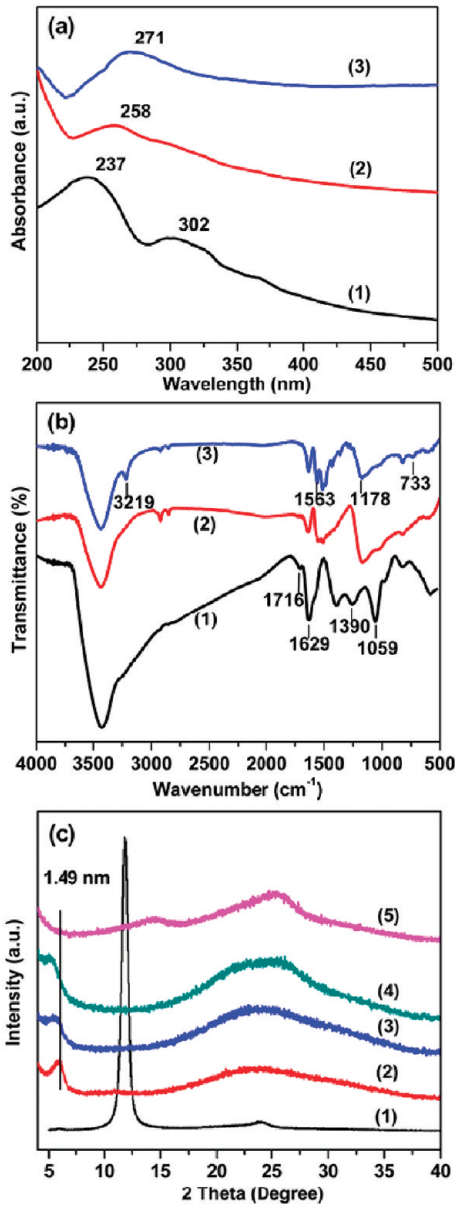

Figure 2. (a) UV−vis absorption spectra of (1) GO, (2) GO-PPD-15 min, and (3) GO-PPD-3 h; (b) FTIR spectra of (1) GO, (2) GO-PPD-15 min, and (3) GO-PPD-3 h; (c) XRD pattern of (1) GO, (2) GO-PPD-15 min, (3) GO-PPD-30 min, (4) GO-PPD-3 h, and (5) GO-PPD-3 h in the absence of NH_3.

CO−H; while the bands at 1716, 1629, and 1059 cm^{-1} are due to C═O in carboxyl group, C═C in aromatic ring, and C−O−C in epoxide group, respectively. After the reaction with PPD, the characteristic absorption bands of −OH, −COOH, and −C−O−C− of GO decreased (both for 15 min and 3 h reaction time), implying the magnitude of reduction. Furthermore, a new peak at 1178 cm^{-1} (C−N stretching vibration) appeared, indicating the formation of C−NH−C bands due to the chemical grafting of PPD to GO surface via nucleophilic substitution reaction between the amine group of PPD and the epoxide group of GO. This conclusion is also supported by the presence of new peaks of deformation and stretching of N−H in $-C-NH_2$ groups at 733 and 1563 cm^{-1}, and the peak of H-bond interaction between $-NH_2$ and oxygen-containing groups of GO at 3219 cm^{-1}.

dx.doi.org/10.1021/am201654b | ACS Appl. Mater. Interfaces 2012, 4, 1948−1953

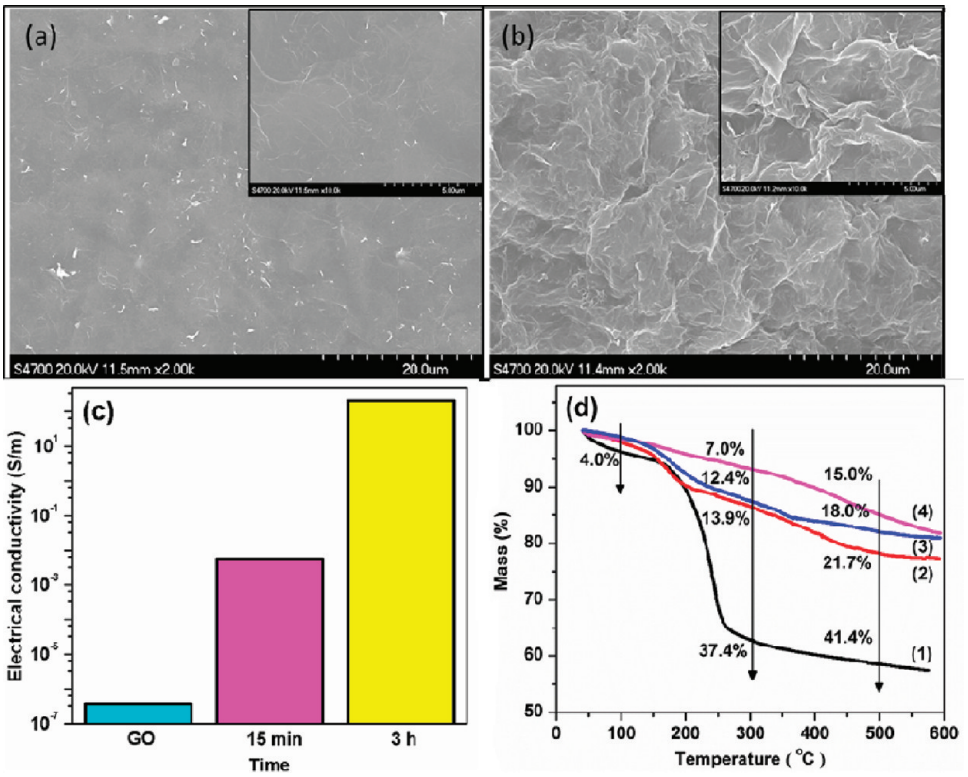

Figure 3. SEM images of (a) GO and (b) GO-PPD-3 h films; (c) electrical conductivities of GO, GO-PPD-15 min, and GO-PPD-3 h films; (d) normalized TGA curves of (1) GO, (2) GO-PPD-15 min, (3) GO-PPD-3 h in the absence of NH_3, and (4) GO-PPD-3 h.

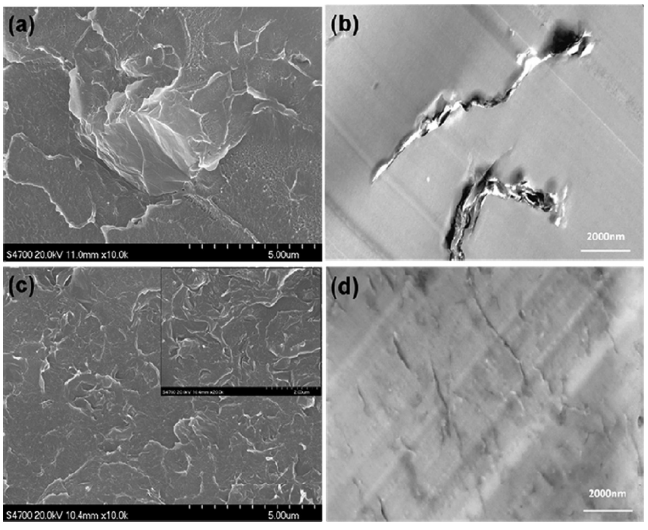

Figure 4. SEM photographs of (a) PS/3 wt % GO and (c) PS/3 wt % GO-PPD composites; TEM photographs of (b) PS/3 wt % GO and (d) PS/3 wt % GO-PPD composites.

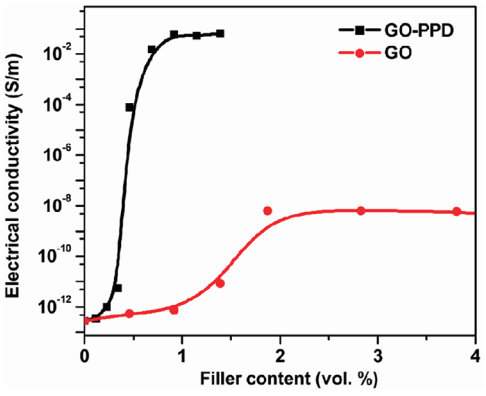

Figure 5. Electrical conductivity of PS/GO and PS/GO-PPD composites as a function of filler content.

Furthermore, the functionalization of GO with PPD is well-reflected in its XRD pattern (Figure 2c). The characteristic diffraction peak of GO is at 11.8° corresponding to an interlayer distance of 0.75 nm. This value is significantly larger than that of pristine graphite (~0.34 nm) because of the introduction of oxygenated functional groups on carbon sheets.[20] Compared to GO, GO-PPD exhibits a diffraction peak at smaller diffraction angle of ~5.9° (d_{001} = 1.49 nm) suggesting a significant enlargement in interlayer spacing,[23] which is attributed to the chemical grafting of PPD onto GO via nucleophilic substitution reaction.[18,24] The following equation can be used to predict the theoretical value of interlayer spacing: $d_{001} = T_{GO} + T_C$, where T_{GO} is the thickness of the GO layer and T_c is the length of the rigid PPD chain.[17,25] The theoretically predicted length of the PPD chain ($l = l\cos 72° + 2L_{C-N}$) was 0.47 nm (Scheme S1, in the Supporting Information). If the average thickness of GO layer of 0.89 nm is used, d_{001} is calculated to be 1.36 nm, which is a little lower than the experimental value (1.49 nm). The differences between the two values are due to the existence of some other structures (see Scheme S1 in the Supporting Information). In addition, a broad peak at ~24.1° appears, that may be due to the restacking of the exfoliated and modified graphene sheets.[26] As for the GO-PPD-3 h specimen without NH_3, its XRD pattern exhibits a peak at 14.5°, much larger than ~5.9° of GO-PPD-3 h with NH_3 solution, implying that the presence of NH_3 provides an alkaline environment that is

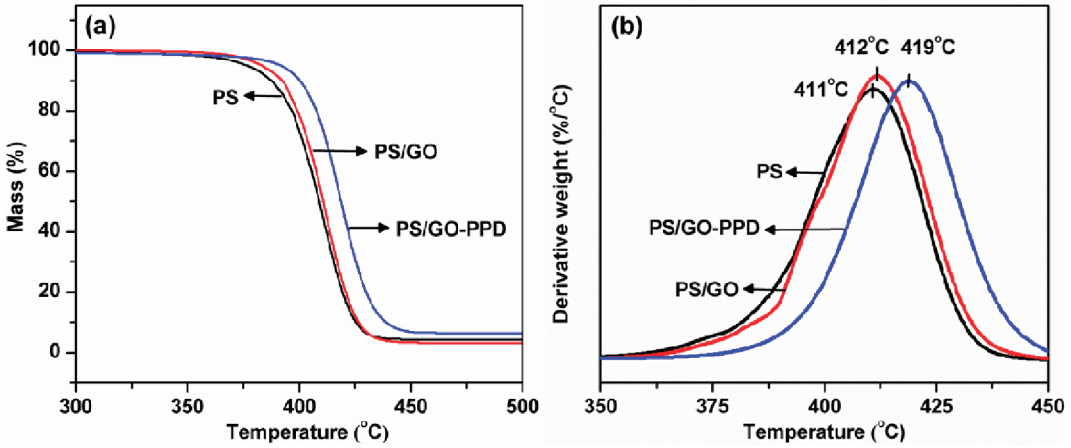

Figure 6. (a) TGA and (b) differential thermogravimetry curves of PS, PS/2 wt % GO and PS/2 wt % GO-PPD-3 h composites.

beneficial to the nucleophilic substitution reaction between GO and PPD. Similar observation was reported by others as well.[27]

Morphology, Electrical Conductivity, and Thermal Stability of GO-PPD. GO and GO-PPD films were prepared by vacuum filtration through porous PP membranes. A striking difference between GO and GO-PPD films is their roughness. The surface of GO film is fairly smooth (Figure 3a) compared to GO-PPD film (Figure 3b). In line with the previous work,[16] this is believed to be due to the presence of rigid phenyl groups of PPD that act as covalently linked nanoscale spacers impeding the face-to-face stacking of GO sheets. Because of the chemical reduction with PPD in the presence of ammonia solution, the electrical conductivity of GO-PPD with refluxing time of 3 h reaches 2.1×10^2 S/m (Figure 3c), which is much higher than that (1.2×10^{-4} S/m) of GO-ODA.[18]

Also, the functionalization and reduction of GO with PPD improves the thermal stability of GO (Figure 3d). For GO, there is a small mass loss (4.0 wt %) around 100 °C due to the loss of adsorbed water and a main mass loss of 37.4 wt % around 300 °C owing to the decomposition of the labile oxygen functional groups, yielding CO_2, CO and vapor. The final mass loss is 41.4 wt % at 500 °C because of the removal of more stable oxygen functionalities.[26] However, for GO-PPD materials, the final mass losses at 500 °C are 21.7 and 15.0 wt %, respectively, for 15 min and 3 h reaction times. Even at 300 °C, compared to 37.4 wt % mass loss of GO, for GO-PPD-3 h it is only 7.0 wt %. These results clearly suggest that GO-PPD materials possess higher thermal stability than GO. Moreover, the mass loss of GO-PPD-3 h in the absence of NH_3 solution at 300 °C is 12.4 wt %, much larger than that of GO-PPD-3 h with NH_3 solution. This indicates that the addition of NH_3 solution is favorable for improving the deoxygenation of GO.

Electrical Conductivity and Thermal Stability of PS Composites. The dispersion quality of GO and GO-PPD was observed with SEM and TEM (Figure 4). Because of the polar mismatch of GO and PS, dispersion of GO is poor in PS matrix, evidenced by the presence of large aggregates (Figure 4a, b). However, GO-PPD exhibits a greatly improved dispersion in PS matrix (Figure 4c, d), which is attributed to benzene group of PPD improving the compatibility of GO-PPD with PS.

GO-PPD is also very efficient in improving the electrical conductivity of PS as indicated by a sharp transition of conductivity with a small percolation threshold of ~0.34 vol % (Figure 5). This is even lower than that of PS/GO-ODA composites, which showed a threshold of 0.45 vol %.[18] The addition of ~0.69 vol % GO-PPD endows PS with an electrical conductivity as high as $\sim 2.0 \times 10^{-2}$ S/m, which is sufficient for many electrical applications,[28] although it is slightly lower than that of functionalized graphene/PS system (~0.1 S/m with 1 vol %).[3] Nevertheless, the simultaneous surface functionalization and reduction approach is advantageous in the production of conductive graphene composites over conventional separate functionalization and reduction methods.

The advantage of GO-PPD over GO is also reflected in thermal stability of PS. Figure 6 shows the TGA results of PS/GO and PS/GO-PPD composites. It is evident that maximum decomposition temperature of the PS/GO composite is only 1 °C higher than that of neat PS; in contrast, it is 8 °C higher for PS/GO-PPD composites because of the improved compatibility between PS and GO-PPD.[29]

CONCLUSION

GO was reduced and functionalized simultaneously by simple refluxing with PPD in the presence of NH_3 solution. The functionalization of GO with PPD substantially enlarged the interlayer spacing of GO sheets, which effectively prevented their aggregation after reduction. The addition of NH_3 solution provided an alkaline environment that was favorable for the reduction and nucleophilic substitution reaction between amine groups of PPD and epoxide groups of GO. The electrical conductivity of GO-PPD was greatly improved to 2.1×10^2 S/m, nearly 9 orders of magnitude higher than that of GO. Also, GO-PPD was efficient in improving the electrical conductivity of PS, leading to a sharp conductivity transition with a low percolation threshold, which is a direct result of the improved dispersion and reduction of GO-PPD compared to GO. The thermal stability of the PS/GO-PPD composite was also higher than that of the PS/GO composite.

ASSOCIATED CONTENT

Supporting Information

Protocols used to synthesize graphene oxide, AFM image of the as-exfoliated GO suspension, and a simple model based on amination of the epoxide groups of GO for the insertion of the amine molecules in the interlayer zone of GO (PDF). This material is available free of charge via the Internet at http://pubs.acs.org.

AUTHOR INFORMATION

Corresponding Author

*E-mail: yuzz@mail.buct.edu.cn (Z.-Z.Y.); aravind@ntu.edu.sg (A.D.).

Notes

The authors declare no competing financial interest.

ACKNOWLEDGMENTS

Financial support from the National Natural Science Foundation of China (51073012, 51125010) and the Program for New Century Excellent Talents in Universities, Ministry of Education of China (NCET-08-0711) are gratefully acknowledged.

REFERENCES

(1) Kim, H.; Miura, Y.; Macosko, C. W. *Chem. Mater.* **2010**, *22*, 3441−3450.
(2) Yoonessi, M.; Gaier, J. R. *ACS Nano* **2010**, *4*, 7211−7220.
(3) Stankovich, S.; Dikin, D. A.; Dommett, G. H. B.; Kohlhaas, K. M.; Zimney, E. J.; Stach, E. A.; Piner, R. D.; Nguyen, S. T.; Ruoff, R. S. *Nature* **2006**, *442*, 282−286.
(4) Balandin, A. A.; Ghosh, S.; Bao, W. Z.; Calizo, I.; Teweldebrhan, D.; Miao, F.; Lau, C. N. *Nano Lett.* **2008**, *8*, 902−907.
(5) Yu, A. P.; Ramesh, P.; Itkis, M. E.; Bekyarova, E.; Haddon, R. C. *J. Phys. Chem. C* **2007**, *111*, 7565−7569.
(6) Yu, A. P.; Ramesh, P.; Sun, X. B.; Bekyarova, E.; Itkis, M. E.; Haddon, R. C. *Adv. Mater.* **2008**, *20*, 4740−4744.
(7) Rafiee, M. A.; Rafiee, J.; Wang, Z.; Song, H. H.; Yu, Z. Z.; Koratkar, N. *ACS Nano* **2009**, *3*, 3884−3890.
(8) Rafiee, M. A.; Rafiee, J.; Srivastava, I.; Wang, Z.; Song, H. H.; Yu, Z. Z.; Koratkar, N. *Small* **2010**, *6*, 179−183.
(9) Novoselov, K. S.; Geim, A. K.; Morozov, S. V.; Jiang, D.; Zhang, Y.; Dubonos, S. V.; Grigorieva, I. V.; Firsov, A. A. *Science* **2004**, *306*, 666−669.
(10) Li, X. S.; Cai, W. W.; An, J. H.; Kim, S.; Nah, J.; Yang, D. X.; Piner, R.; Velamakanni, A.; Jung, I.; Tutuc, E.; Banerjee, S. K.; Colombo, L.; Ruoff, R. S. *Science* **2009**, *324*, 1312−1314.
(11) Kim, K. S.; Zhao, Y.; Jang, H.; Lee, S. Y.; Kim, J. M.; Kim, K. S.; Ahn, J. H.; Kim, P.; Choi, J. Y.; Hong, B. H. *Nature* **2009**, *457*, 706−710.
(12) Berger, C.; Song, Z. M.; Li, T. B.; Li, X. B.; Ogbazghi, A. Y.; Feng, R.; Dai, Z. T.; Marchenkov, A. N.; Conrad, E. H.; First, P. N.; de Heer, W. A. *J. Phys. Chem. B* **2004**, *108*, 19912−19916.
(13) Chen, Y.; Zhang, X.; Yu, P.; Ma, Y. W. *Chem. Commun.* **2009**, *30*, 4527−4529.
(14) Stankovich, S.; Dikin, D. A.; Piner, R. D.; Kohlhaas, K. A.; Kleinhammes, A.; Jia, Y.; Wu, Y.; Nguyen, S. T.; Ruoff, R. S. *Carbon* **2007**, *45*, 1558−1565.
(15) Xu, L. Q.; Yang, W. J.; Neoh, K. G.; Kang, E. T.; Fu, G. D. *Macromolecules* **2010**, *43*, 8336−8339.
(16) Zhang, D. D.; Zu, S. Z.; Han, B. H. *Carbon* **2009**, *47*, 2993−3000.
(17) Herrera-Alonso, M.; Abdala, A. A.; McAllister, M. J.; Aksay, I. A.; Prud'homme, R. K. *Langmuir* **2007**, *23*, 10644−10649.
(18) Li, W. J.; Tang, X. Z.; Zhang, H. B.; Jiang, Z. G.; Yu, Z. Z.; Du, X. S.; Mai, Y. W. *Carbon* **2011**, *49*, 4724−4730.
(19) Zhang, H. B.; Zheng, W. G.; Yan, Q.; Yang, Y.; Wang, J. W.; Lu, Z. H.; Ji, G. Y.; Yu, Z. Z. *Polymer* **2010**, *51*, 1191−1196.
(20) Schniepp, H. C.; Li, J. L.; McAllister, M. J.; Sai, H.; Herrera-Alonso, M.; Adamson, D. H.; Prud'homme, R. K.; Car, R.; Saville, D. A.; Aksay, I. A. *J. Phys. Chem. B* **2006**, *110*, 8535−8539.
(21) Paredes, J. I.; Villar-Rodil, S.; Martinez-Alonso, A.; Tascon, J. M. D. *Langmuir* **2008**, *24*, 10560−10564.
(22) Zhao, X.; Zhang, Q. H.; Chen, D. J.; Lu, P. *Macromolecules* **2010**, *43*, 2357−2363.
(23) Huang, Y. L.; Tien, H. W.; Ma, C. C. M.; Yang, S. Y.; Wu, S. Y.; Liu, H. Y.; Mai, Y. W. *J. Mater. Chem.* **2011**, *21*, 18236−18241.
(24) Yang, H. F.; Shan, C. S.; Li, F. H.; Han, D. X.; Zhang, Q. X.; Niu, L. *Chem. Commun.* **2009**, *26*, 3880−3882.
(25) Bourlinos, A. B.; Gournis, D.; Petridis, D.; Szabo, T.; Szeri, A.; Dekany, I. *Langmuir* **2003**, *19*, 6050−6055.
(26) Zhou, T. N.; Chen, F.; Liu, K.; Deng, H.; Zhang, Q.; Feng, J. W.; Fu, Q. A. *Nanotechnol.* **2011**, *22*, 045704.
(27) Zhu, C. Z.; Guo, S. J.; Fang, Y. X.; Dong, S. J. *ACS Nano* **2010**, *4*, 2429−2437.
(28) Chung, D. D. L. *J. Mater. Sci.* **2004**, *39*, 2645−2661.
(29) Yang, X. M.; Li, L. A.; Shang, S. M.; Tao, X. M. *Polymer* **2010**, *51*, 3431−3435.